JOURNAL OF THERMOPHYSICS AND HEAT TRANSFER
Vol. 15, No. 2, April–June 2001

Thermal Contact Conductance of Metal/Polymer Joints: An Analytical and Experimental Investigation

J. J. Fuller* and E. E. Marotta†
Clemson University, Clemson, South Carolina 29634-0921

The heat flow across a metal/polymer interface is a very important problem in many modern engineering applications. A thermal joint conductance model that employs the surface mechanics of a contact interface in conjunction with an existing elastic thermal contact conductance model was developed. In developing the model, an elastic contact hardness term was derived to predict the actual contact area of a metal/polymer interface under loading. The model predicts a microscopic resistance region where the interface resistance is dominant and a bulk resistance region where the thermal conductivity of the polymer is dominant. An experimental apparatus was fabricated, and a successful experimental program was conducted. New experimental data were gathered on different polymeric specimens over a pressure range of 138–2758 kPa (20–400 psi). The experimental data were compared to the proposed thermal joint conductance model. It was found that the proposed model predicted the data quite well. The data followed the predicted trends for both the microscopic and bulk resistance regions.

Nomenclature

A_a = apparent area of contact, m^2
A_r = real area of contact, m^2
a_c = contact radius, m
a_0 = Hertzian contact radius, m
c = half-width of plane contact area, m
E' = effective elastic modulus $(E_1 E_2)/[(E_2(1-\nu_1^2) + E_1(1-\nu_2^2)]$, Pa
E_p = elastic modulus of polymer, Pa
E_s = elastic modulus of substrate, Pa
H_c = contact microhardness, Pa
H_e = Mikic elastic hardness $(E'/\sqrt{2})\times$ m, Pa
H_{ep} = polymer elastic hardness, Pa
h_{bulk} = thermal bulk conductance, W/m^2 K
h_c = thermal contact conductance, W/m^2 K
h_e = dimensionless elastic conductance
h_j = thermal joint conductance, W/m^2 K
$h_{j\,exp}$ = experimentally calculated joint conductance, W/m^2 K
h_{micro} = thermal microscopic conductance, W/m^2 K
$J(t)$ = creep compliance
k_{flux} = thermal conductivity of flux meter, W/m K
k_p = thermal conductivity of polymer, W/m K
k_s = harmonic mean thermal conductivity, W/m K
L = load, N
m_{ab} = mean absolute asperity slope, rad
n = number of contact spots per unit area of apparent contact, m^{-2}
P = apparent pressure, Pa
P/H_c = dimensionless plastic contact pressure
P/H_e = dimensionless elastic contact pressure
P_m = mean pressure at interface, Pa
Q = heat rate, W
q = heat flux through flux meter, W/m^2
R_b = bulk thermal resistance, K/W
$R_{g,1}$ = gap resistance at interface 1, K/W
$R_{g,2}$ = gap resistance at interface 2, K/W
R_j = joint resistance, K/W
R_{micro} = microscopic thermal resistance, K/W
$R_{t,c}$ = contact resistance, K/W
R_1 = thermal resistance for upper interface, K/W
R_2 = thermal resistance for lower interface, K/W
T_c = temperature of specimen, K
T_{sl} = temperature of lower interface of specimen, K
T_{su} = temperature of upper interface of specimen, K
T_1 = temperature at surface 1, K
T_2 = temperature at surface 2, K
t = elastic layer (polymer) thickness, m
t_f = polymer thickness after loading, m
t_0 = polymer thickness before loading, m
t^* = critical polymer thickness, m
Y = separation distance between contacting surfaces, m
$Y(t)$ = relaxation modulus
ε_p = strain on polymer in the vertical direction
λ = dimensionless separation distance, Y/σ
ν_p = Poisson's ratio of polymer
ν_s = Poisson's ratio of substrate
ρ = radius of curvature of asperity, m
σ = rms roughness, m
σ_t = polymer tensile strength, Pa

Presented as Paper 2000-0877 at the AIAA 38th Aerospace Sciences Meeting, Reno, NV, 10–14 January 2000; received 5 May 2000; revision received 4 December 2000; accepted for publication 15 December 2000.

*Research Assistant, Mechanical Engineering Department. Member AIAA.
†Assistant Professor, Mechanical Engineering Department. Member AIAA.

Introduction

WHENEVER thermal energy flows across an interface, there exists an opposition to that flow of thermal energy. This opposition is analogous to electrical resistance and is thus called the *thermal resistance.* When the heat flow is across two surfaces in contact, the opposition is defined as the thermal contact resistance. The thermal contact resistance is measured by determining the heat rate across the two contacting surfaces and the difference between the respective surface temperatures:

$$R_{t,c} = (T_1 - T_2)/Q \tag{1}$$

Thermal contact resistance plays a major role in almost all power-generating systems. Many design constraints are based on heat generation and the ability of a system to effectively dissipate the generated heat. Quantifying the heat flow can be a very difficult problem in many electronic applications.

Computer chip-packaging technology is a good example of the desire for maximum heat dissipation over a small area. As the circuit densities continue to increase in electronic devices, greater importance is being placed on the ability of a chip-packaging configuration to dissipate heat. In a personal communication B. T. Han,

E. E. Marotta, and J. M. Ochterbeck have proposed several possible chip-packaging configurations. It is critical that the computer chip remains cooler than its recommended operating temperature or premature chip failure will likely occur.

To allow the packaging configuration to quickly dissipate more heat, heat sinks or heat pipes are commonly employed. The heat must flow from the chip through the adhesive or interstitial material to the heat sink or spreader and then to the ambient air. At each interface a contact resistance opposes the heat flow. If the contact resistance can be reduced or eliminated, the effective thermal conductance of the configuration can be increased. As the contact resistance is lowered, the thermal conductance is increased, and thus more heat is dissipated. A very important interface in chip packaging occurs when a metal and a polymeric interstitial material are in contact.

Currently, there are many models to predict the contact conductance of a metal/metal interface, but Marotta and Fletcher[1] showed that discrepancies can exist when these models are applied to a metal/polymer interface. Modeling a metal/polymer interface thermally is a very challenging problem because of the nature of the intrinsic mechanical properties of polymers.

A metal/metal interface is usually modeled as two interfaces having an equivalent roughness where asperity deformation occurs against a rigid, smooth surface. However, when dealing with a metal/polymer interface the previous model may not be valid because a polymer behaves like an elastic layer. A metal/polymer interface can be modeled as a rigid metal indentor in contact with a softer elastic layer.

Background Information: Polymers

Polymers are manufactured for their properties and are comprised of organic chain-like molecules. Polymers are being used more and more in everyday items including adhesives, coatings, plastics, rubber products, and many other applications. Polymers are usually classified by their mechanical and thermal behavior into the following three categories: thermoplastic, thermoset, and elastomers.[2]

Flexibly linked and branched molecular chains usually describe the class of thermoplastic polymers. Thermoplastic polymers are comprised of individual monomers, and they typically exhibit ductile properties. Thermosets are comprised of a more cross-linked, rigid network of molecular chains, which make them generally stronger, harder, and more brittle than either thermoplastic or elastomeric polymers. The final group of polymers, elastomers, is comprised of lightly cross-linked chains. Elastomers have the intrinsic ability to elastically deform under large strains.

Thermoplastic and elastomeric polymers are especially interesting because they exhibit viscoelastic behavior, and this behavior can make it difficult to quantify a polymer's mechanical properties. Viscoelastic behavior is defined by the fact that a polymer's mechanical properties, such as elastic modulus, bulk modulus, shear modulus, Poisson's ratio, may be a function of time and temperature. Flügge[3] has mathematically defined a relaxation modulus $Y(t)$ and creep compliance $J(t)$ to quantify the viscoelastic behavior.

Krevelen[4] defines the following five temperature controlled regions of elastic behavior: glassy ($T \leq T_g$, E constant), transition region ($T \approx T_g$, E varies with temperature), rubbery ($E \approx$ constant again), rubbery flow, and liquid flow. Knowing the current temperature of a polymer is very important in understanding the mechanical properties of that polymer. If a polymer remains below its glass transition temperature, the mechanical properties of the polymer will remain constant with time.

Problem Statement

Increasingly, organic interstitial materials, such as elastomers, are being employed to a greater extent in power generating systems, and with greater use follow an increased interest in the thermal transport properties of these polymers. These properties include thermal conductivity, thermal diffusivity, and the thermal contact conductance at the interface with other materials. One very important consideration, where limited knowledge exists, is the flow of heat across a metal/polymer interface. Currently, a usable and verifiable model does not exist for predicting the thermal performance of metal/polymer joints.

The scope of this investigation will be limited first to conforming rough surfaces, which are nominally flat, at a uniform interface pressure (load/apparent area) and then to the class of thermoplastic and elastomeric polymers. Thermoset polymers tend to behave in a more hard and brittle manner than the usually soft and ductile thermoplastics and elastomers. The soft and ductile behavior of thermoplastic and elastomeric polymers are what make the contact resistance between a metal and a polymer an interesting yet challenging problem.

Literature Review

Metal/Metal Thermal Contact Models

Sridhar and Yovanovich[5] presented a critical review of the currently accepted thermal contact conductance models for rough conforming surfaces in contact under a known load. When modeling a contact interface, the following three types of components are needed: a thermal component, a surface geometry component, and a surface deformation component. A contact conductance model requires a thermal model to predict the conductance, which in turn uses a surface geometry and surface deformation model to predict the actual contact area. According to the authors, the major difference among contact conductance models is the surface geometry chosen.

Cooper et al.[6] (CMY) were able to define the thermal model, for appropriately distributed contacts, to predict the thermal contact conductance:

$$h_c = \frac{2k_s n a_c}{(1 - \sqrt{A_r/A_a})^{1.5}} \tag{2}$$

where the terms for contact spot radius a_c, number of contact spots n, and the ratio of real to apparent area A_r/A_a are defined by using the appropriate surface geometry and deformation model.

When defining the surface geometry model for conforming rough surfaces, it is generally accepted to assume a circular contact spot and then use probability theory to predict the number and size of these contact spots. There are commonly used deformation models that can be employed: the Hertz elastic model[7] or the geometric plastic model. Depending on which deformation model is chosen, the thermal contact conductance model becomes either a plastic or an elastic thermal contact model.[5]

For this investigation it was decided that two thermal contact conductance models would be of critical importance and warranted further study. Therefore, the CMY[6] plastic model and the Mikic[8] elastic model are reviewed here.

The CMY[6] model was defined for conforming rough surface where the asperities undergo a plastic deformation under loading and follow a Gaussian distribution of asperity heights. The authors used geometrical parameters such as surface roughness and mean profile slope to predict the actual contact area. The model is defined by the following equations[5]:

$$\lambda = \sqrt{2} erfc^{-1}\left(\frac{2P}{H_c}\right) \tag{3}$$

$$h_c = \frac{k_s}{2\sqrt{2\pi}} \frac{m_{ab}}{\sigma} \frac{\exp(-\lambda^2/2)}{\left[1 - \sqrt{\frac{1}{2} erfc(\lambda/\sqrt{2})}\right]^{1.5}} \tag{4}$$

The authors reduced the analytical equations (3) and (4) to the following dimensionless thermal contact conductance correlation equation:

$$h_c \sigma / k_s m_{ab} = 1.45(P/H_c)^{0.985} \tag{5}$$

Yovanovich[9] proposed a slight modification of the CMY model with the following correlation equation, which was obtained from fully rederived analytical expressions:

$$h_c \sigma / k_s m_{ab} = 1.25(P/H_c)^{0.95} \tag{6}$$

Based on the foundation laid by the CMY model, Mikic[8] derived an elastic thermal contact model. The model assumes the case of rough nominally flat surfaces in contact with circular contact points. Using Hertzian contact analysis,[10] he found that the elastic contact area is exactly half the plastic contact area. The Mikic[8] elastic model is defined by the following equations[5]:

$$H_e = \frac{E' m_{ab}}{\sqrt{2}} \tag{7}$$

$$\lambda = \sqrt{2} erfc^{-1}\left(\frac{4p}{H_e}\right) \tag{8}$$

$$h_c = \frac{k_s}{4\sqrt{\pi}} \frac{m_{ab}}{\sigma} \frac{\exp(-\lambda^2/2)}{\left[1 - \sqrt{\frac{1}{4} erfc(\lambda/\sqrt{2})}\right]^{1.5}} \tag{9}$$

The elastic contact hardness defines the elastic area of contact as proportional to the load for metal/metal contacts assuming asperity contact on a rigid flat surface where only the asperity deforms. Again, the analytical equatons were then reduced to the following dimensionless thermal contact conductance correlation:

$$h_c \sigma / k_s m_{ab} = 1.55(P\sqrt{2}/E' m_{ab})^{0.94} \tag{10}$$

Other elastic deformation models reviewed by Sridhar and Yovanovich[5] were the Greenwood and Williamson[11] elastic model; the Bush et al.[12] asymptotic elastic model, which is valid only when $\lambda \geq 2$; and the Whitehouse and Archard[13] elastic model, which differs by assuming asperity peaks that do not follow a Gaussian distribution and peak curvatures that have a distribution, which are dependent on their heights.

Metal/Polymer Contact Models

Meijers[14] studied the contact problem of a rigid cylinder indenting an elastic layer resting on a rigid base. The analysis assumed plane deformation and frictionless contact between the cylinder and the elastic layer. Asymptotic solutions are presented for the following two cases: when the ratio of the half-width c of the contact area to the thickness of the layer t is small and when the ratio of the contact radius to the thickness c/t is large. Solutions are presented for all values of A_r/t and for a layer Poisson's ratio between 0 and 0.5.

Chen and Engel[15] conducted an impact and contact stress analysis of multilayer media. They reformulated the mixed boundary value problem using general approximation techniques that were solvable using numeric calculations. They compared their analysis to other exact solutions and reported good agreement. Numerical results were presented for surface pressure, contact radius, and penetration depth for both a parabolic and circular flat-ended punch. The authors also compared their analysis to experimental data gathered by dropping a steel ball onto nylon and rubber layers over a granite base. Again, a good agreement was found between the analytical solutions and experimental results. For the analysis of the parabolic punch, the authors assumed a spherical body of radius ρ, where $\rho \gg a_c$.

Jaffar[16] developed a numerical scheme for solving axisymmetric contact problems involving a rigid indentor on an elastic layer. He assumed a frictionless contact and derived solutions for both bonded and unbonded elastic layers. He categorized the indention of an elastic layer into two classes. The first class is defined by complete contact, where the radius of the contact region is known, for example a flat-ended circular punch. The second class is defined by incomplete contact, where the radius of contact is not known a priori, for example a spherical punch. Jaffar presented solution plots for the pressure distribution, penetration depth, and normal surface displacement for both spherical and flat-ended circular punches for a_c/t in the range of $0 \leq a_c/t \leq 20$ and $0 \leq \nu \leq 0.5$.

Matthewson[17] was able to develop closed-form solutions for axisymmetric contact on thin compliant coatings. The author assumed a thin layer bonded to a rigid substrate, a frictionless contact, and for the thin layer to behave linearly elastic under loading. The Young's modulus of the elastic layer was assumed to be small when compared with the Young's modulus of the indentor and underlying substrate. Matthewson was able to derive solutions for the following three cases: indention of the layer by a spherical tipped indentor, where $\rho \gg a_c$; indention by a blunt cone, where $\nu = 0.5$; and for an indentor of arbitrary profile, where $\nu = 0.5$. An experimental program was conducted and data gathered for the cases of indention by the spherical tipped indentor and blunt cone. The model seemed to predict the data well with an average difference reported of 5%.

Metal/Polymer Thermal Contact Conductance Data

Mirmira et al.[18] conducted an experimental investigation measuring the thermal contact conductance of a wide range of commercially available elastomeric gaskets. The experimental investigation was conducted with the elastomeric gaskets maintained at mean interface temperatures of 20 and 80°C and over a mean interface pressure range of 172–6900 kPa (25–1000 psi). The thermal contact conductance for the elastomeric gaskets ranged from 150 to 13500 W/m^2 K. From analysis of the data, the authors concluded that the mean interface temperature did not affect the thermal conductance of the gaskets, but slightly higher conductance values were recorded for higher pressures.

Quillet et al.[19] studied the thermal characteristics of a metal/polymer interface during injection molding processes. The experimental investigation dynamically measured the thermal contact resistance of acrylonitrile-butadiene-styrene during the injection molding process and determined how temperature and time affected the thermal contact resistance during injection molding. The authors defined a methodology for simultaneously measuring the thermal contact resistance and the temperature field in the polymer. Their results modeled the transient contact resistance during injection molding. Their results are not applicable to the current study because steady-state conditions are assumed in the current study.

Narh and Sridhar[20] measured the joint thermal resistance of polystyrene as a function of thickness at constant temperature and pressure. The amount of data presented was very limited. The authors proposed a correlation that is seemingly a modification of CMY[6] model, but it was not specified whether the elastic or plastic contact deformation assumption a priori was employed. Also, the model contained many material constants, which were not given. Thus, this cannot be compared to other published data. The authors did conclude that an important parameter in dealing with polymers might be the temperature.

Parihar and Wright[21] studied the thermal contact resistance and total resistance of a (SS304)/silicone rubber/(SS304) joint under light loads (0.02–0.25 MPa of apparent stress) and different applied heat fluxes. Because different polymers can be difficult to compare because of their different properties, this paper also seeks to suggest a standard procedure for the measurement of the thermal contact resistance at the metal/elastomer interface. The paper reflects on some of the vast difficulties that are faced when modeling the metal/polymer interface.

A limited amount of data was presented showing the change in contact resistance caused by variations in temperature and mean pressure at the interface. An important observation, reported by the authors, was that the specimen's surface characteristics were not affected by the experimentally applied conditions of time, heat, and load. They concluded that the bulk resistance could play a large role in the joint resistance depending on the specimen's thickness. Also, in their measurements the authors found that the thermal contact resistance varied between the hot and cold interfaces with the hot thermal interface resistance being greater than the cold thermal interface resistance by a factor of 1.3–1.6. The authors attributed this increase in resistance to a high thermal rectification caused by the heat flux lines constricting when entering the polymer but then expanding when leaving the polymer.

Marotta and Fletcher[1] measured the thermal conductivity and the thermal contact conductance of several widely available thermoplastic and thermosetting polymers. The thermal conductivity data were obtained over a temperature range of 10–100°C, and the thermal contact conductance data were obtained over a pressure range

of 510–2760 kPa (75–400 psi) and a temperature range of 20–40°C. The authors then compared the experimentally measured data to current thermal contact models developed for metal/metal contacts, such as the elastic contact model developed by Mikic[8] and the plastic contact model developed by CMY.[6] The Mikic[8] and CMY[6] models are accepted and proven for metal/metal contacts; however, Marotta and Fletcher[1] observed that a thermal model was needed for accurately predicting the joint conductance of metal/polymer junctions. The model should account for both the microscopic contact resistance and the bulk thermal resistance of the polymer layer along with polymer deformation effects.

Analytical Model

The analytical model will encompass a range of light to moderate loading pressures (138–2758 kPa or 20–400 psi) at the contact interface because this is the range of pressures where metal and polymers are in contact in most modern engineering applications. In dealing with the contact of a hard metal into a much softer elastic layer, a different approach was taken than for metal/metal contacts. To make the model as accurate as possible, the proposed model was developed using an existing elastic conductance model modified with surface contact mechanics principles that incorporated the polymer's material properties.

In bare metal to metal contacts, the real contact area is always less than the apparent contact area A_a. Because thermoplastic and elastomeric polymers have a comparatively lower modulus of elasticity, the calculated real contact area can actually be greater than the apparent area. Physically, the metal asperities will tend to have little or no deformation while the softer polymer material will "envelop" and wrap around the metal asperities.

In relation to the thermal contact conductance, this increase in contact area as it approaches and then becomes greater than the apparent contact area will cause the contact resistance to become negligible. As the load increases, so does the real contact area, which causes the interface resistance to become negligible while the bulk thermal properties of the polymer begin to dominate. This type of contact mechanics behavior of the interface is the reason a joint conductance was chosen to be included in the model. A joint conductance model will be able to incorporate the microscopic resistance at low loads, both the microscopic and bulk resistance at intermediate loads, and then just the bulk resistance at the higher loads.

The present analytical investigation involves the use of four common polymers previously studied by Marotta and Fletcher[1] (delrin, Teflon®, polycarbonate, and polyvinyl chloride). These polymers were chosen based on their commercial importance in current engineering applications and the availability of their material properties from standard chemical handbooks. The four polymers also displayed a range of Young's modulus between 5.52×10^8 and 4.14×10^9 Pa.

In addition, for the present investigation the mode of deformation between the metal and the softer polymer is assumed to be elastic during light to moderate loading. This assumption is supported by the experimental study conducted by Parihar and Wright,[21] which measured the rms roughness and the asperity slope of the steel flux meters and the silicone specimen before and after loading. The measured values were almost the same before and after loading, which they concluded implies elastic deformation at the interface.

Critical Thickness

An important parameter to note is the thickness of the elastic layer t. Because the polymer layer is usually in contact with a much harder underlying substrate, the substrate could affect the contact mechanics of the metal/polymer joint. It is desired to know above what critical thickness the elastic layer becomes independent of the influence of the underlying rigid substrate.

Makushkin[22] studied the influence of the underlying substrate and the thickness of an elastic layer during spherical indentor penetration. He derived a mathematical expression for the critical polymer layer thickness t^* beyond which the substrate will not influence the deformation of the elastic layer. The expression for the critical thickness was defined as

$$t^* = 16.8\left(\frac{\sigma_t \rho}{E_p}\right)\left(\frac{(E_p/E_s)^{0.11}}{\upsilon_p^{0.41}\upsilon_s^{0.003}}\right) \tag{11}$$

Using the surface properties reported by Marotta and Fletcher,[1] the critical polymer thickness, for the four selected polymers employed by them, was calculated and is shown here: Teflon, 80.0; Delrin, 26.1; PVC, 17.2; and Poly, 28.2. It was observed that only for very thin layers would the underlying substrate affect the deformation. The thickness of the polymers employed by Marotta and Fletcher[1] ranged from 1.65 to 12.7 mm, which is well above the calculated critical polymer thickness for the respective polymer. The present experimental investigation will maintain all of the specimen's thickness around 1 mm to ensure that the underlying substrate will not influence the deformation.

Contact Modeling of the Polymer/Metal Interface

The contact mechanics of the interface were modeled by the assumption of a rigid sphere impacting an elastic layer. Finkin[23] investigated the determination of the Young's modulus of rubber sheets by the indentation of a spherically tipped indentor. Finkin's work is based on the assumption of a thick elastic layer where the thickness is greater than the radius of contact. He based his experiments on the analytical contact mechanics studies conducted by Vorovich and Ustinov.[24] They solved the mathematical problem of a rigid sphere contacting an elastic layer on a rigid half-space. They determined the contact radius in terms of an asymptotic power series of nondimensionalized layer thickness as

$$\frac{a_c}{t} = \frac{a_0}{t} - 0.113\left(\frac{a_0}{t}\right)^4 + 0.114\left(\frac{a_0}{t}\right)^6 + 0.025\left(\frac{a_0}{t}\right)^7 - 0.004\left(\frac{a_0}{t}\right)^8 \tag{12}$$

where a_0 represents the contact radius predicted by the Hertz solution and is defined as

$$a_0 = \left[\frac{3L\rho\left(1-\upsilon_p^2\right)}{4E_p}\right]^{\frac{1}{3}} \tag{13}$$

The desire was to first develop a mathematical expression that calculated the contact radius in a more easily applied equation while also obtaining a nondimensional expression for the applied load. The Buckingham Pi Theorem was employed to obtain an expression for the contact radius as a function of polymer thickness, load, asperity radius of curvature, and the Young's modulus.

It was observed that the polymer layer's dimensionless contact radius a_c/t was a function of dimensionless load $E_p t^3/\rho L$. The dimensionless contact radius was plotted as a function of the new dimensionless load parameter for a range of thickness reported by Marotta and Fletcher.[1] As desired, the new dimensionless load parameter produced one curve regardless of E_p, t, or polymer. Finally, to verify that the equation was independent for a range of polymer materials, four different polymers were plotted as shown in Fig. 1. A curve fit equation was obtained and defined as

$$a_c/t = 0.857\left(\rho L / E_p t^3\right)^{\frac{1}{3}} \tag{14}$$

Because the test specimens used by Marotta and Fletcher[1] were relatively thick (1.5 mm), it is not suprising that Eq. (14) represents the Hertzian solution from Eq. (13). The only difference between Eqs. (14) and (13) is the load term in Eq. (13), which has been replaced by an average polymer Poission's ratio of 0.4.

It was now desired to know for what range of interface load and specimen thickness would the Hertzian solution be applicable. It was known that under a high load and/or a small layer thickness the Hertzian solution would fail because of the high strains that the elastic layer would experience. Figure 2 shows a plot of dimensionless contact radius [Eq. (12)] vs dimensionless load. As one can see, when the dimensionless load remains above 0.7, the contact radius

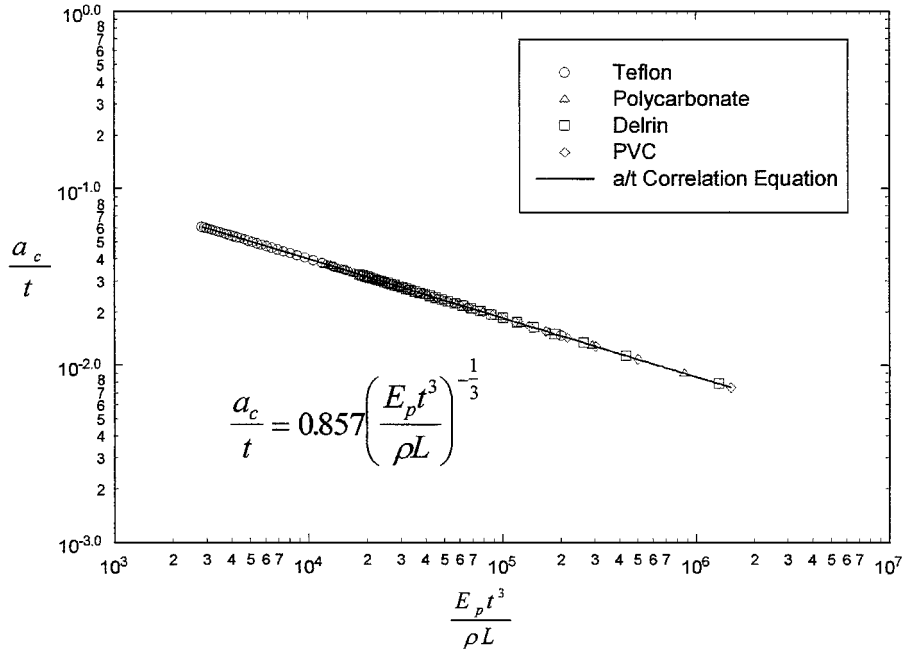

Fig. 1 Dimensionless contact radius as a function of dimensionless load for selected polymers.

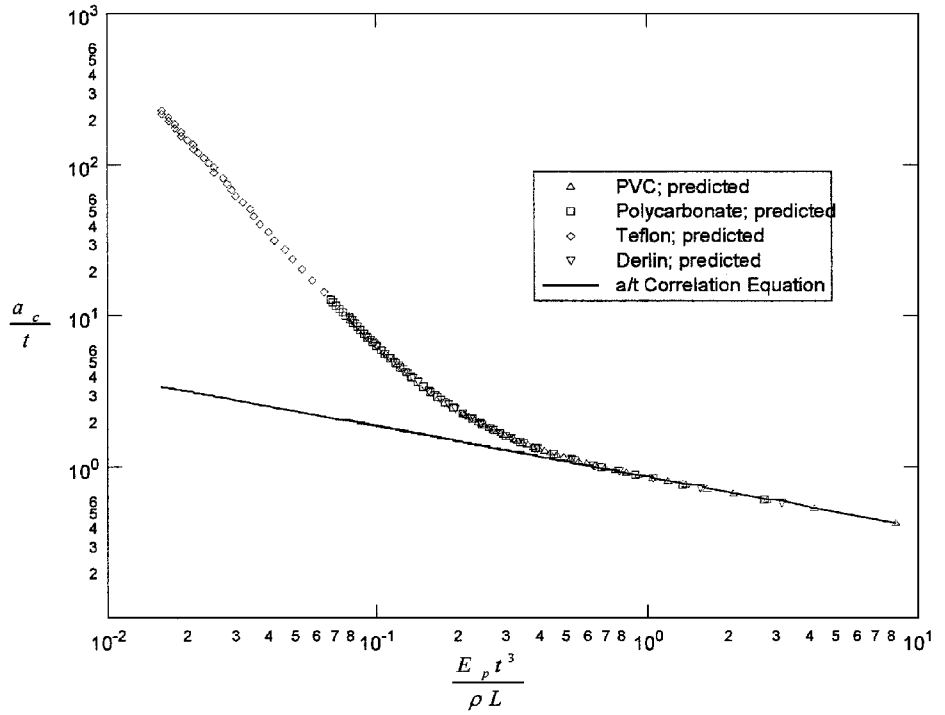

Fig. 2 Plot of Vorovich and Ustinov's[24] equation with correlation equation: dimensionless contact radius as a function of dimensionless load.

for a rigid indentor into an elastic layer can be modeled using the Hertzian solution. The calculated critical load of the four selected polymers assuming a specimen thickness of 1 mm is shown here: Teflon, 1.10×10^5; Delrin, 7.14×10^5; PVC, 8.23×10^5; and poly, 4.73×10^5. It was noticed that only for extremely high interface pressures would Hertzian contact analysis not be valid.

The fact that the contact radius can be modeled by the Hertzian solution is very important because it validates using an existing thermal contact model that is based on Hertzian analysis. However, a modification to the elastic hardness parameter must be made to accommodate polymer layers.

Thermal Joint Resistance Model

The joint resistance to heat flow that incorporates the bulk properties of the polymer layer can be defined as

$$R_j = R_{\text{micro},1} + R_{\text{bulk}} + R_{\text{micro},2} \tag{15}$$

By redefining the resistance as

$$R_j = 1/h_j A \tag{16}$$

$$R_{\text{micro},i} = (1/h_{\text{micro},i} A) \qquad i \to 1 \text{ to } 2 \tag{17}$$

$$R_{\text{bulk}} = 1/h_{\text{bulk}} A \tag{18}$$

Eq. (15) can be rewritten in terms of thermal conductance as

$$h_j = 1/(1/h_{\text{micro},1} + 1/h_{\text{bulk}} + 1/h_{\text{micro},2}) \tag{19}$$

A general diagram of the modeled joint conductance terms, for which Eq. (19) applies, is shown in Fig. 3 (modeled after that found in Ref. 25).

Microscopic Conductance Model

Once it had been ascertained that the polymer layer would deform independently of the underlying substrate, the next step was to define the microscopic and bulk thermal resistance. A possible candidate for defining the microscopic resistance was the established Mikic[8] elastic model for thermal contact conductance already reviewed in this paper.

The Mikic[8] model assumes elastic deformation of the contacting asperities onto a rigid flat surface. However, this is not the case for metal/polymer contacts. Instead, the metal/polymer interface was modeled as a rigid indentor contacting an elastic surface. Therefore, to incorporate Mikic's model a "polymer elastic contact hardness" (H_{ep}) had to be defined to replace the term H_e for metal/metal contacts.

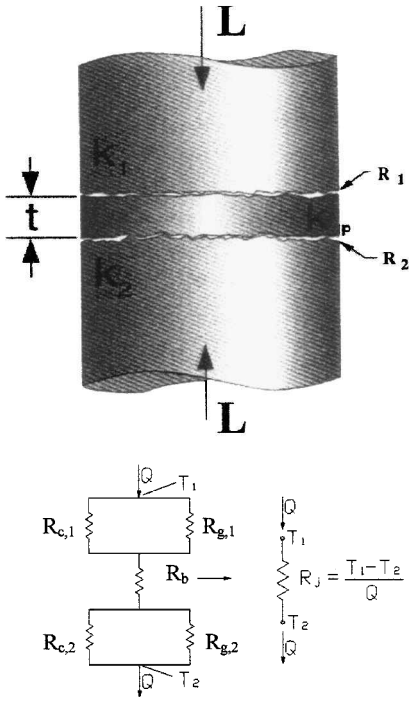

Fig. 3 General diagram of the modeled joint conductance (after Yovanovich et al.[25]).

By assuming a Gaussian distribution of asperity heights, Greenwood and Williamson[11] showed that the area of contact of nominally flat surfaces is almost exactly proportional to the load. They defined an elastic contact hardness that controls the area of contact as

$$H_{\text{elastic}} = CE'm_{\text{ab}} \tag{20}$$

where C is a constant found by plotting dimensionless mean pressure vs dimensionless load as shown in Fig. 4.

For metal/polymer interfaces employed in this investigation, the constant was found to be approximately 0.433; therefore, a polymer elastic hardness was able to be defined as

$$H_{\text{ep}} = E_p m_{\text{ab}}/2.3 \tag{21}$$

By inserting the new polymer elastic hardness into the analytical model represented by Eqs. (8) and (9), a predictive model for the microscopic contact conductance was obtained. Figure 5 shows a plot of the dimensionless contact conductance as a function of dimensionless interface pressure incorporating the polymer elastic hardness. From the plot of the analytical solution, a simple correlation for the dimensionless contact conductance was obtained:

$$\frac{h_{\text{micro}}\sigma}{k_s m_{\text{ab}}} = 1.49\left(\frac{2.3P}{E_p m_{\text{ab}}}\right)^{0.935} \tag{22}$$

from which h_{micro} can be calculated.

Bulk Thermal Conductance

The next step was to derive an expression for the bulk resistance of the polymer layer that includes the compressibility effects of the polymer.

The bulk thermal conductance of a polymer layer can be defined as

$$h_{\text{bulk}} = k_p/t_f \tag{23}$$

Because the polymer is modeled as an elastic and compressible layer, the thickness would be a function of load. The change in thickness can be defined as

$$\Delta t = t_0 - t_f \tag{24}$$

Applying Hook's law and the assumption of linear elasticity, there is only stress in the vertical direction, and this stress is equal to the applied pressure P, which implies that

$$\varepsilon_p = P/E_p \tag{25}$$

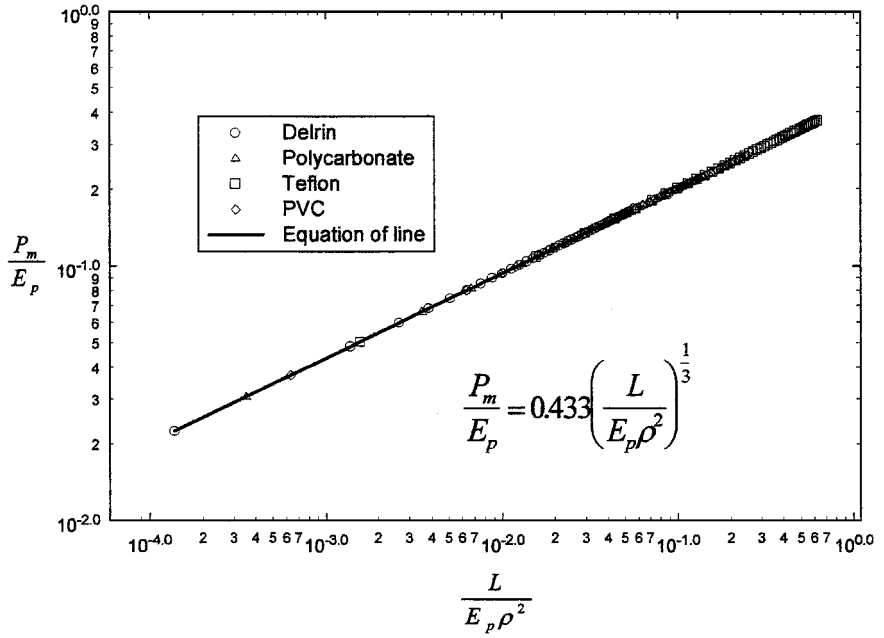

Fig. 4 Dimensionless mean pressure as a function of dimensionless load for selected polymers.

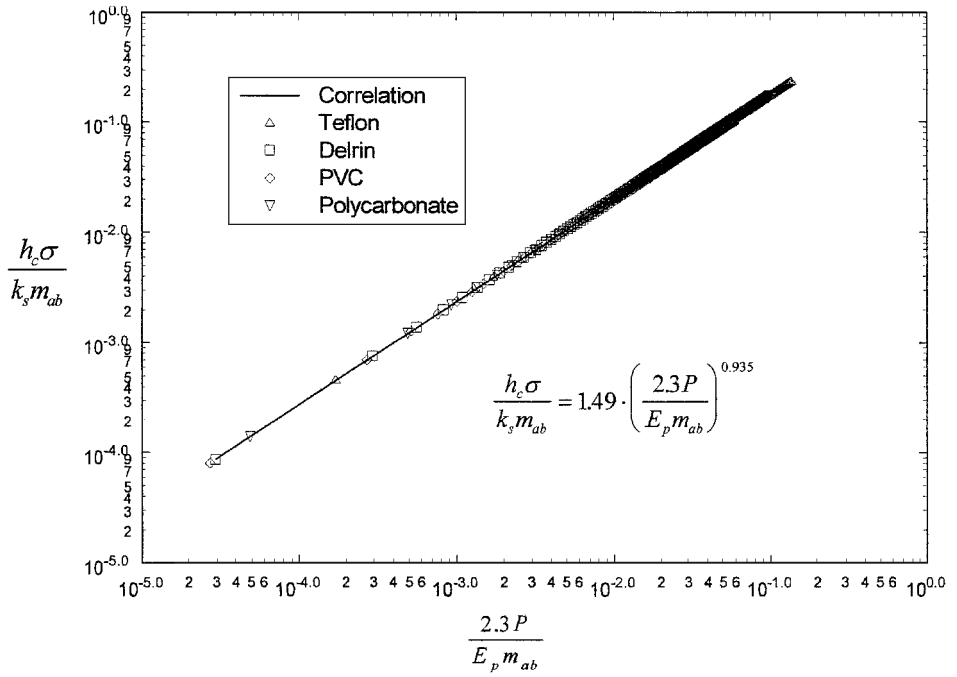

Fig. 5 Dimensionless contact conductance as a function of dimensionless pressure for selected polymers: correlation (Fuller and Marotta[30]).

Incorporation of Eq. (25) into the expression for the final layer thickness (24) results in the following expression:

$$t_f = t_0(1 - P/E_p) \tag{26}$$

It was observed that only for polymers with low Young's modulus ($<2.5 \times 10^7$ Pa) and high pressures ($>3.0 \times 10^6$ Pa) will the final thickness change by more than 12%. By substituting Eq. (26) into Eq. (23), an expression for the bulk conductance h_{bulk} was defined that included the one-dimensional, compressibility effects of the elastic layer.

$$h_{\text{bulk}} = k_p/t_0(1 - P/E_p) \tag{27}$$

Thermal Joint Conductance Model

Now that an equation has been derived for both the microscopic and bulk conductance, a final joint conductance model was defined as

$$h_j = 1/[1/h_{\text{micro},1} + t_0(1 - P/E_p)/k_p + 1/h_{\text{micro},2}] \tag{28}$$

where $h_{\text{micro},i}$ was defined by Eq. (22). The proposed joint conductance model predicts that the contact resistance will be dominant at lower pressures and that the bulk resistance will dominate at the higher pressures.

Experimental Investigation

Once a model had been developed, it was desired to validate the model by comparing the predicted values with experimentally gathered thermal joint conductance data. Because very little data have been published on the joint conductance values of metal/polymer joints, it was decided that a new experimental program should be undertaken. The purpose of the experimental program was to validate the new joint conductance model by obtaining new experimental data, especially in the range of light to moderate interface pressures.

Experimental Facility

To obtain experimental data on the polymers of interest, an experimental program was conducted similar to that of Marotta and Fletcher.[1] A diagram of the experimental apparatus is shown in Fig. 6.

The experimental apparatus was housed in a vacuum bell and maintained at a low pressure of 1 Pa (1×10^{-5} bar) using a Welch

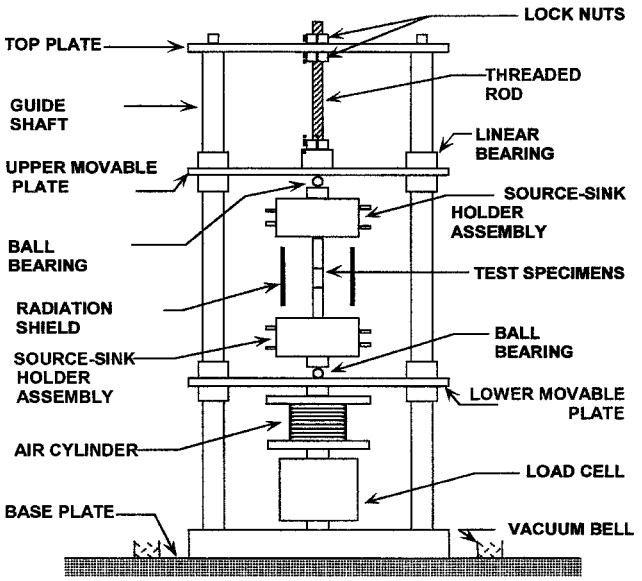

Fig. 6 Experimental facility.

Duo-Seal® rotary vacuum pump. The pressure was monitored using a pressure transducer connected to an Alcatel TA111 indicator.

The experimental apparatus consists of a vertical stack that contains three vertical stainless-steel columns mounted with two movable Teflon plates on linear bearings. An applied load to the experimental stack was controlled using a Bimba Flat-1® air cylinder, and the applied load was measured using an OMEGA LCHD-1K low profile load cell wired to an OMEGA DP41-S high-performance strain gauge indicator. Uniform loading of the test section was ensured by the use of two hardened stainless-steel balls that transferred the load from the vertical column to the source/sink assemblies.

The experimental stack consisted of an upper flux meter, polymer specimen, and a lower flux meter. A diagram of the experimental stack is shown in Fig. 7. Both stainless-steel and Al 6061 flux meters were used. Each flux meter was housed in a fabricated source/sink holder. A Watlow Thinband® 500-W band heater encompassed the upper source holder. The lower sink holder was cooled by a glycol/water solution supplied by a constant temperature chiller. By

Table 1 Material characteristics

Parameter	UPPER Al flux meter	Delrin 1	Delrin 2	Poly	PVC
t_0, mm	——	1.274	1.322	1.440	1.313
σ, m	5.11×10^{-7}	2.13×10^{-6}	2.23×10^{-6}	6.32×10^{-7}	5.35×10^{-7}
m_p, rad	0.2667	0.6257	0.5696	0.4227	0.3997
k, W/m-K	183.02	0.38[a]	0.38[a]	0.22[a]	0.17[a]
E, Pa	7.20×10^{10}	3.59×10^{9}	3.59×10^{9}	2.38×10^{9}	4.14×10^{9}

[a]Marotta and Fletcher.[1]

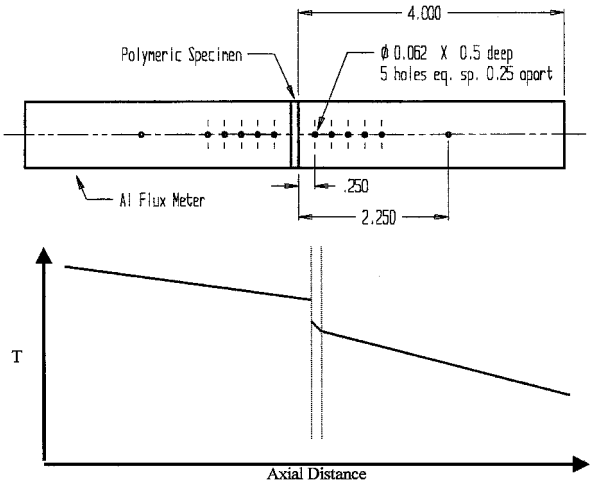

Fig. 7 Schematic of the experimental stack with polymeric specimen.

controlling the voltage to the band heater and the temperature of the chiller solution, a desired specimen average temperature could be achieved. A radiation shield also surrounded the experimental stack to minimize radiation losses and ensure one-dimensional conduction through the experimental stack.

The thermal conductivity of the 6061 Al flux meters was calibrated by using National Institute of Standards and Technology (NIST) iron samples. A 1-in. specimen was machined from the same bar stock the flux meters were machined and tested to obtained the thermal conductivity as a function of temperature.

Sample Preparation

The flux meters and the polymer specimens were all cut to a diameter of 2.54 cm (1 in.). The Al flux meters were equipped with six and the stainless-steel flux meters were equipped with five 30 gauge "special limit of error" T-type thermocouples that were placed at the centerline.

The polymeric specimens were first machined into 2.54-cm-diam rods. A Buehler ISOMET 2000 cutting tool was used to cut specimens to approximately 2-mm thickness. To ensure a nominally flat surface, both surfaces of the specimens were then polished using an EXAKT grinding wheel. The thickness of the specimens was measured at five different locations to ensure an uncertainty in the thickness of ± 0.005 mm.

The surface characteristics (rms roughness and average asperity slope) of the flux meters and polymeric specimens were measured using a WYKO NT-2000 noncontact surface profilometer with a magnification of 50×. Measurements were taken at five different positions on the surface and then averaged to ensure uniformity of the values. Material characteristics for the Al flux meter and the polymeric specimens are shown in Table 1.

Experimental Procedure

Joint conductance values were measured between the flux meters and the polymer specimens over an interface pressure range of 138–2758 kPa (20–400 psi). The average specimen temperature of the polymeric specimens was maintained at 40°C (±1°C) throughout the experiments.

To measure the joint conductance, a polymer specimen was placed between the two flux meters. Air was allowed into the air cylinder until the experimental stack (upper flux meter, specimen, lower flux meter) was vertically aligned with the specimen in light contact with both flux meters. Because only the microscopic resistance at the upper face of the specimen was considered, Dow Corning 340 heat sink compound was applied between the lower flux meter and the lower specimen interface. This allowed the contact resistance at the lower specimen interface to be neglected.

Once the experimental stack was correctly aligned, air was allowed into the air cylinder until the desired starting apparent pressure of 138 kPa was acting on the polymer specimen. Next, the chiller was set to 5°C, and the voltage supplied to the band heater was increased until an average temperature of 40°C was achieved between the interface of the polymer specimen and the upper flux meter. The temperatures through the flux meters were measured and recorded using a National Instruments (NI) SCXI hardware and NI Lab View data acquisition setup.

Because it was desired to know the joint conductance values as a function of apparent pressure, the pressure on the polymeric specimens was varied. For each specimen the joint conductance was measured at 68.9 kPa (10 psi) increments from 138–689 kPa (20–100 psi), 138 kPa increments (20 psi) from 689–1379 kPa (100–200 psi), and 345 kPa (50 psi) from 1379–2758 kPa (200–400 psi). The average temperature across the upper specimen interface was also monitored through the entire process to ensure a value of 40°C.

To obtain a joint conductance measurement, the specimen was allowed to settle at the desired pressure until steady state had been reached. Steady state was considered to be achieved when the average temperature of the interface did not change more that ±0.2°C over a 30-min period. Once sufficient time had been allowed for the system to reach steady state, the data acquisition was stopped, and the joint conductance values were averaged over the 30-min period. Next, the pressure inside the air cylinder was increased until the next desired pressure was reached. The process was repeated until the final apparent pressure of 2758 kPa was reached.

Calculations

The thermocouples placed in the Al flux meters were used to calculate the heat flux into and out of the polymer specimen. The temperature at each thermocouple location was then recorded, and a sum of least-squares method was used to extrapolate the temperature at the interface of each of the flux meters. The temperatures were then averaged to obtain an average temperature across the upper interface.

The joint conductance was calculated by defining the joint conductance [Eq. (29)] and Fourier's law [Eq. (30)]:

$$h_{j\,\mathrm{exp}} = \frac{q_{\mathrm{flux}}}{T_{\mathrm{su}} - T_{\mathrm{sl}}} \tag{29}$$

$$q_{\mathrm{flux}} = k_{\mathrm{flux}} \frac{\Delta T_{\mathrm{flux}}}{\Delta x_{\mathrm{flux}}} \tag{30}$$

The thermal conductivity k_{flux} was calculated by averaging the six thermocouples in the flux meter and inputting the calculated average temperature into the thermal conductivity equation of aluminum (Al) as a function of temperature. To reduce the experimental uncertainty, the temperature difference term ΔT_{flux} was defined

by the difference in the temperature between the thermocouple at location one and the thermocouple at location six. Finally, Δx_{flux} was defined as the distance between the thermcouples at location one and six, respectively.

Uncertainty Analysis

The techniques set forth by Kline and McClintock[26] were used to determine an overall experimental uncertainty of the measured joint conductance values. The uncertainties of the various values used to calculate the joint conductance were combined to determine an overall experimental uncertainty. A complete explanation of the uncertainty analysis was presented by Fuller.[27]

The uncertainty of the experimentally measured joint conductance values consisted of the uncertainty in the thermal conductivity of the 6061 Al flux meters, the temperatures recorded within the flux meters, the measured distance between the thermocouple locations, and the calculated interface temperature of the upper and lower flux meters.

The uncertainty of the thermal conductivity of the 6061 Al flux meters was comprised of the following uncertainties: the thermal conductivity of the NIST iron flux meters (3% above 280 K), the temperature gradient within the NIST flux meters (2%), the temperature gradient within the Al test specimen (5%), and the measured distance between the thermocouple locations within both the NIST flux meters and the Al test specimen (1.6%). The uncertainty of the thermal conductivity of the 6061Al flux meters was calculated to be 6.6%.

The total average uncertainty of the experimental joint conductance values was 17%. The experimental uncertainty was largely due to calculation of the temperature gradient through the Al flux meters (15%). Also contributing were the uncertainties of the thermal conductivity of the Al flux meters (6.6%), the measured distance between the thermocouple locations in the flux meters (0.8%), and the extrapolated temperature at the upper and lower specimen interfaces (0.6%).

Results and Discussion

Data were obtained on five polymer specimens, previously stated in Table 1, over a pressure range of 138–2758 kPa. It was desired to see how well the proposed joint conductance model predicted the experimental data.

Results from Experimental Program

The data were gathered with thermal grease applied to contact surface 2 and vacuum conditions. The thermal grease allowed for almost total area contact between the polymer and the metal thus causing the $1/h_{\text{micro},2}$ term to be negligible. Therefore, the joint conductance model can be reduced to the following expression:

$$h_j = 1/[1/h_{\text{micro},1} + t_0(1 - P/E_p)/k_p] \tag{31}$$

Equation (31) was employed for comparison of the thermal joint conductance model to the experimental data.

The joint conductance as a function of interface pressure for the polycarbonate specimen is shown in Fig. 8. The specimen had a nominal thickness of 1.44 mm, and the thermal conductivity of polycarbonate was measured by Marotta and Fletcher[1] to be 0.22 W/m-K. The glass transition temperature for polycarbonate is 145°C[5]. Because the specimen was maintained below the glass transition temperature, the Young's modulus should not be a strong function of time.

The joint conductance for the polycarbonate specimen follows the predicted trend. The joint conductance is lowest at the lowest pressures and is a function of the interface pressure until the bulk conductance becomes dominant. It appears from the plotted data that 800 kPa (≈120 psi) is the approximate threshold pressure beyond which the microscopic resistance is negligible and only the bulk resistance is apparent. Therefore, after the apparent interface pressure reaches 800 kPa the joint conductance is no longer a function of the interface pressure and remains constant with increasing pressure.

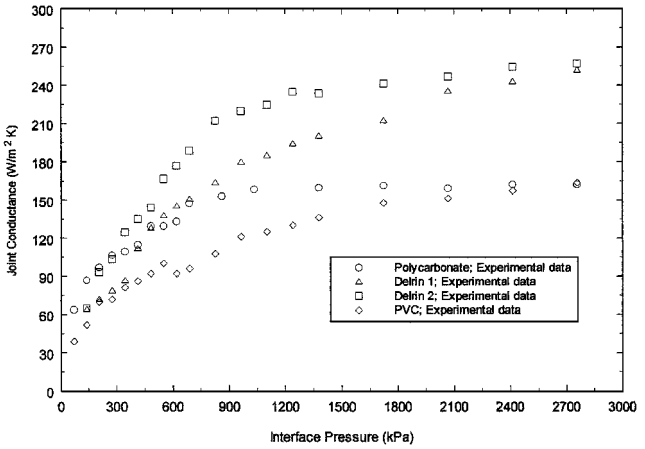

Fig. 8 Experimental joint conductance data.

Two Delrin specimens were also tested. They were both prepared from the same stock and varied in thickness and surface properties. Marotta and Fletcher[1] measured the thermal conductivity of Delrin to be 0.38 W/m-K. The glass transition temperature of Delrin is −85°C[3], which implies that the Delrin specimen could exhibit viscoelastic behavior (Young's modulus could be a function of time).

The joint conductance as a function of interface pressure for the first Delrin specimen tested, Delrin 1, is also shown in Fig. 8. The specimen had a nominal thickness of 1.27 mm. The data for Delrin 1 falls in the midrange where both the microscopic and bulk resistances are important. Throughout the pressure range the joint conductance for Delrin is a function of the interface pressure. The data indicate that after 2000 kPa (≈300 psi) the joint conductance may reach an asymptotic line.

The joint conductance as a function of interface pressure for Delrin 2 is shown in Fig. 8. The specimen had a nominal thickness of 1.32 mm. The experimental data for Delrin 2 follow the predicted trend of an increasing joint conductance with pressure and then leveling off to a bulk value. As expected, the data show a leveling of the joint conductance values at 1100 kPa (≈160 psi) after which the joint conductance value was independent of pressure.

The joint conductance as a function of interface pressure for the polyvinyl chloride (PVC) specimen is shown in Fig. 8. The specimen had a nominal thickness of 1.14 mm, and Marotta and Fletcher[1] measured the thermal conductivity to be 0.17 W/m-K. The glass transition temperature of PVC is 175°C[3]. Like polycarbonate, because the average specimen temperature was kept well below the glass transition temperature of PVC, the specimen is outside of the viscoelastic range. Thus, the PVC specimen's Young's modulus should not be a function of time.

Again, the joint conductance for the PVC specimen follows the anticipated trend. The joint conductance increases linearly and then asymptotically with increasing interface pressure to a bulk conductance value. From the plotted data it appears that the joint conductance of the PVC specimen is almost constant after 1400 kPa (≈1200 psi).

Next, the experimental data were compared to the proposed joint conductance model with plots of the experimental joint conductance data of the Delrin, polycarbonate, and PVC specimens with predicted values. The dimensionless joint conductance is plotted as a function of the dimensionless pressure is shown in Fig. 9.

Although the average temperature of the Delrin specimens was maintained within the viscoelastic range for the polymer, there was not a noticeable deviation from the predicted values. Presently, the proposed joint conductance model does not account for viscoelastic behavior, yet at least for Delrin it does not seem to have a large influence.

The joint conductance model seems to predict reasonably well the experimentally gathered data, and only a few points deviate from

Table 2 Selected percent difference of predicted vs measured joint conductance values

Specimen	Exp. 30 psi, W/m^2 K	Pred. 30 psi, W/m^2 K	% Diff.	Exp. 400 psi, W/m^2 K	Pred. 400 psi, W/m^2 K	% Diff.
Delrin 1	71.8	85.1	−16.9	251.6	244.0	3.1
Delrin 2	93.0	83.0	11.4	256.0	234.9	8.6
PVC	67.2	70.9	−5.4	146.8	135.9	7.7
Polycarbonate	97.0	97.3	−0.3	162.2	145.6	10.8

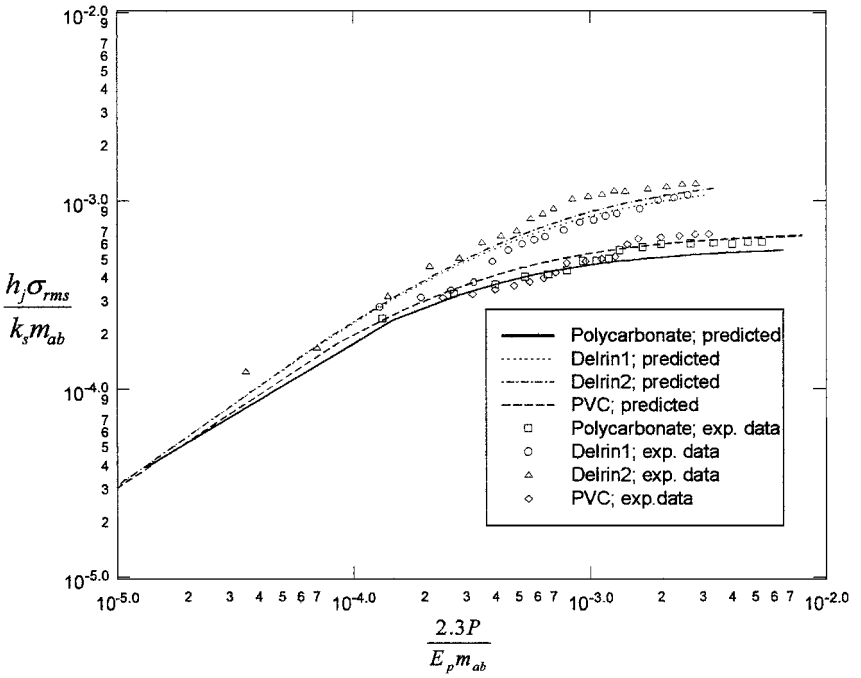

Fig. 9 Dimensionless joint conductance as a function of dimensionless pressure; predicted values with experimental data.

the predictive curves. Table 2 tabulates the difference between the predicted and experimentally measured joint conductance values for pressures of 206 kPa (30 psi) and 2758 kPa (400 psi) for the polymer specimens employed in the study. All tabulated values for the difference between model prediction and experimental data are within the computed experimental uncertainty of 17%. Therefore, the model agrees quite well with the experimental data.

Areas for Future Study

The proposed joint conductance model and experimental program were a good first study of the joint conductance of a metal/polymer joint; however, there are still many areas that could warrant further research and study.

It is desired to have an empirical expression relating the Young's modulus of a polymer as a function of time. Vettegren et al.[28] and Bronnikov et al.[29] developed an expression that relates the time and temperature dependent Young's modulus to the material properties of a polymer before loading. Once validated, the empirical expression could be easily incorporated into the joint conductance model, and then the joint conductance model would account for the viscoelastic behavior of polymers.

Another area warranting further study is the pressure distribution at the metal/polymer interface. The current model assumes a uniform pressure distribution across the interface. In many electronics applications, because of mismatched coefficients of thermal expansion, a nonuniform pressure distribution may be created across the interface. Once a contact geometry can be defined, it is possible to define the pressure distribution as a function of the distance from the centerline and then incorporate that function into the joint conductance model.

The thermal joint conductance model was developed for vacuum conditions, which is the case for satellite and space applications. A final area of study would be investigating a metal/polymer joint under atmospheric conditions. The presence of air at the interface would provide a second avenue for heat flow through the interface. An additional conduction term could easily be added in parallel to the microscopic resistance. The decreased total would account for the heat flow across a gas-filled gap.

Conclusions

An analytical thermal conductance model has been developed, and an experimental investigation has been conducted. A thermal joint conductance model was developed using contact mechanics principles and basic material properties to predict the thermal conductance of metal/polymer joints, and an experimental program was conducted. The data were compared to the joint conductance model, and good agreement was found between the data and predicted values.

A thermal joint conductance model has been developed and verified for predicting the joint conductance across metal/polymer joints. The model was developed using limiting assumptions to make an initial model practical and verifiable. This joint conductance model should form the foundation for future and expanded research on the heat flow through metal/polymer joints.

References

[1] Marotta, E. E., and Fletcher, L. S., "Thermal Contact Conductance of Selected Polymeric Materials," *Journal of Thermophysics and Heat Transfer*, Vol. 20, No. 2, 1996, pp. 334–342.

[2] Askeland, D. R., *The Science and Engineering of Materials*, 3rd ed., PWS Publishing Company, Inc., Boston, 1994.

[3] Flügge, W., *Viscoelasticity*, Blaisdell, Waltham, MA, 1967, pp. 22–24.

[4] Krevelen, D. W. Van, *Properties of Polymers*, 3rd ed., Elsevier, New York, 1990.

[5] Sridhar, M., and Yovanovich, M., "Review of Elastic and Plastic Thermal Contact Conductance Models: Comparison with Experiment," *Journal of Thermophysics and Heat Transfer*, Vol. 8, No. 4, 1994, pp. 633–640.

[6]Cooper, M., Mikic, B. B., and Yovanovich, M., "Thermal Contact Conductance," *International Journal of Heat and Mass Transfer*, Vol. 12, 1969, pp. 279–300.

[7]Johnson, K. L., *Contact Mechanics*, Cambridge Univ. Press, Cambridge, England, U.K., 1985.

[8]Mikic, B. B., "Thermal Contact Conductance; Theoretical Considerations," *International Journal of Heat and Mass Transfer*, Vol. 17, 1974, pp. 205–214.

[9]Yovanovich, M. M., "New Contact and Gap Conductance Correlations," AIAA Paper 81-1184, June 1981.

[10]Timoshenko, S., and Goodier, J. N., *Theory of Elasticity*, 2nd ed., McGraw–Hill, New York, 1951.

[11]Greenwood, J. A., and Williamson, J. B. P., "Contact of Nominally Flat Surfaces," *Proceedings of the Royal Society of London*, Vol. A295, 1966, pp. 300–319.

[12]Bush, A. W., Gibson, R. D., and Thomas, T. R., "The Elastic Contact of a Rough Surface," *Wear*, Vol. 35, 1975, pp. 87–111.

[13]Whitehouse, D. J., and Archard, J. F., "The Properties of Random Surfaces of Significance in Their Contact," *Proceedings of the Royal Society of London*, Vol. A316, 1970, pp. 97–121.

[14]Meijers, P., "The Contact Problem of a Rigid Cylinder on an Elastic Layer," *Applied Science Research*, Vol. 18, Feb. 1968, pp. 353–383.

[15]Chen, W. T., and Engel, P. A., "Impact and Contact Stress Analysis in Multilayer Media," *International Journal of Solids and Structures*, Vol. 8, 1972, pp. 1257–1281.

[16]Jaffar, M. J., "A Numerical Solution for Axisymmetric Contact Problems Involving Rigid Indenters on Elastic Layers," *Journal of the Mechanics and Physics of Solids*, Vol. 36, No. 4, 1988, pp. 401–416.

[17]Matthewson, M. J., "Axi-Symmetric Contact on Thin Compliant Coatings," *Journal of the Mechanics and Physics of Solids*, Vol. 29, No. 2, 1981, pp. 89–113.

[18]Mirmira, S. R., Marotta, E. E., and Fletcher, L. S., "Thermal Contact Conductance of Elastomeric Gaskets," *Journal of Thermophysics and Heat Transfer*, Vol. 12, No. 3, 1998, pp. 454–456.

[19]Quillet, S., Le Bot, P., Delaunay, D., and Jarny, Y., "Heat Transfer at the Polymer-Metal Interface: A Method of Analysis and Its Application to Injection Molding," *American Society of Mechanical Engineers National Heat Transfer Conference*, Vol. 2, 1997, pp. 9–16.

[20]Narh, K. A., and Sridhar, L., "Measurement and Modeling of Thermal Contact Resistance at a Plastic Metal Interface," ANTEC, 1997, pp. 2273–2277.

[21]Parihar, S. K., and Wright, Neil T., "Thermal Contact Resistance at Elastomer to Metal Interfaces," *International Communications in Heat and Mass Transfer*, Vol. 24, No. 8, 1997, pp. 1083–1092.

[22]Makushkin, A. P., "Study of Stress-Strain of Polymer Layer During Spherical Indenter Penetration," *Trenie I Iznos*, Vol. 5, No. 5, 1984, pp. 823–832.

[23]Finkin, E. E., "The Determination of Young's Modulus from the Indentation of Rubber Sheets by Spherically Tipped Indentors," *Wear*, Vol. 19, 1971, pp. 277–286.

[24]Vorovich, I. I., and Ustinov, Iu. A., "Pressure of a Die on an Elastic Layer of Finite Thickness," *Journal of Applied Mathematics and Mechanics*, Vol. 23, No. 3, 1959, pp. 637–650.

[25]Yovanovich, M. M., Culham, J. R., and Teertstra, P., "Calculating Interface Resistance," *Electronics Cooling*, Vol. 3, No. 2, 1997, pp. 24–29.

[26]Kline, S. J., and McClintock, F. A., "Describing Uncertainties in Single-Sample Experiments," *Mechanical Engineering*, Vol. 75, No. 1, 1953, pp. 3–8.

[27]Fuller, J. J., "Thermal Contact Conductance of Metal/Polymer Joints: An Analytical and Experimental Investigation," M.S. Thesis, Dept. of Mechanical Engineering, Clemson Univ., Clemson, SC, May 2000.

[28]Vettegren, V. I., Bronnikov, S. V., Korzhavin, L. N., and Frenkel, S. Ya., "New Approach to the Description of Young's Modulus for Highly Oriented Polymers. I. Temperature-Time Dependences of Young's Modulus," *Journal of Macromolecular Science—Physics*, Vol. B29, No. 4, 1990, pp. 285–302.

[29]Bronnikov, S. V., Vettegren, V. I., and Frenkel, S. Ya., "New Approach to the Description of Young's Modulus for Highly Oriented Polymers. II Relationship Between Young's Modulus and Thermal Expansion of Polymers over a Wide Temperature Range," *Journal of Macromolecular Science—Physics*, Vol. B32, 1993, pp. 33–50.

[30]Fuller, J., and Marotta, E. E., "Thermal Contact Conductance of Metal/Polymer Interfaces," *Journal of Thermophysics and Heat Transfer*, Vol. 14, No. 2, 2000, pp. 283–286.